



Stockholm
University

Department of Biochemistry and Biophysics

Evaluating the ability of Mutual Information to detect epileptic seizures in EEG data

Johan Eskils

Year 2021

60 HP

Group and supervisor Samuel Flores
Project time 15-01-2020 – 12-01-2021

Abstract	3
Introduction	4
Electroencephalogram (EEG)	5
Mutual Information (MI).....	8
Methods and material.....	9
EEG data	9
Software	10
MI calculation.....	11
Results.....	13
Detection results	15
Discussion.....	24
References	26
Acknowledgement	28

Abstract

Uncontrolled bursts of electrical activity between neurons in the brain are known as a seizure, a physical condition with various symptoms such as convulsions (uncontrollable muscle spasms with loss of consciousness), involuntary stiffness and shaking of the body, confusion, blackouts, loss of bladder control and many more. Individuals suffering from recurring seizures are diagnosed with epilepsy. Predicting or rapidly detecting the onset of a seizure is critical for avoiding neurological damage in epileptic patients. A method that can give a rapid alert for hospital staff will reduce the cost of hospital care and the risk of a patient suffering from physical and neurological injuries.

Mutual Information (MI) is an information-theoretic quantity that can be visually represented in many ways especially with EEG (scalp electroencephalogram) data. Mutual information has the capability of detecting the onset of a seizure and monitor the duration of a seizure visually. MI combined with a peak finding algorithm is not complicated mathematically and is also highly visually interpretable. “The aim of this work was to evaluate whether MI can be used for predicting epileptic seizures using EEG data and to evaluate how well MI can discriminate between data with or without seizures”. Prediction statistics, Accuracy, Specificity, Precision and Selectivity were calculated on a per-second basis for the EEG recordings. Gold Standard Positives were from the published CHB-MIT dataset annotations, while test positives were from a novel rising-edge Mutual Information method. Even if MI has the capability to detect seizures it is vital that it is combined with good rising-edge finding algorithms to screen out peaks originating from other intense brain activity, noise spikes or electrode potential bias in the EEG recordings that may result in false positives. It was found that this method performed well on EEG data; it was better at detecting the onset of seizure (as was our priority), and less effective at identifying the end (or equivalently, the duration) of the seizure.

Introduction

Patients with epilepsy, a central nervous system disorder, suffer from recurrent seizures. A seizure can occur without warning and a constant risk for an epileptic person to enter a state with lost attention and body convulsions which sometimes are mistaken for intoxication. Frequent seizures increase the risk of physical and neurological injuries and even the death of the patient. There are two classes of seizures: A seizure that starts in one area and spreads across the brain depends on the neurons involved are known as focal seizures. The second class the generalized seizure can start as a focal seizure that spreads from one side of the brain to the other or start simultaneously over both sides of the brain [1, 4, 7].

A rapid method for detection of the onset of seizures is important for rapid medical treatment and alerting hospital staff. A skilled Electroencephalographer require 6-10 seconds to determine whether an abnormality in the EEG (scalp electroencephalogram) recording can be considered as a seizure or a part of a seizure [15]. It is of less interest to estimate the duration of a seizure than to detect the onset.

The scalp electroencephalogram (EEG), a non-invasive multi-channel recording of the electrical activity in the brain are interpreted by skilled physicians for detecting seizures. Each channel represents the difference between potentials measured at two electrodes. The electrode positions on the scalp are set by the used international standard. The features in an EEG that indicate a seizure in one individual do not always indicate one in other patients [2, 6, 7, 10, 11, 13, 15]. For this reason seizure detection based on multi-patient data tends to be less accurate than a patient specific method [2, 11, 15]. A screening method that is non-patient specific that rapidly can alert an onset of a seizure from similar EEG pattern is also of value [2, 3, 11, 13].

In this work my aims were to evaluate Mutual Information (MI) an information-theoretic method based on paired observations and its capability to detect and even predict seizures. A rapid method that can discriminate an MI peak due to seizures and from one due to non-seizure events is also important, as there is a lot of non-seizure brain activity that results in high MI. Prompt seizure detection requires peak finding algorithms that identify the rising edge of the peak rather than the peak maximum. MI are a method that can be visually interpreted during the recording of an EEG and provide a lot of information for the doctor monitoring the patient.

Electroencephalogram (EEG)

An EEG (scalp electroencephalogram) recording is characterized by the number of channels and the position of the electrodes. International standards define the naming convention for scalp electrode arrays. The prefix letters **F**, **T**, **C**, **P**, **O** represent to the brain lobes where the electrode is positioned on the scalp.

This is then followed by a suffix. An odd number represents an electrode positioned on the left side of the scalp and an even number an electrode positioned on the right side of the scalp. The suffix letter **z** indicates that the electrode is placed in the midline between hemispheres. The letters represent the lobes as follows **F** the frontal, **T** the temporal, **C** the central, **P** the parietal and **O** the occipital lobe. The raw data in this work were collected from recordings with the 10-20 international system and the locations of the electrodes are shown in figure 1. The sampling frequency of the EEG is not set by a standard. Two electrodes and the measured difference in potential between them defines the EEG channel. The size of the collected data is dependent of the sampling frequency and one hour at 256 Hz result in 921600 data points for each measured EEG channel. An EEG of with one channel is shown in figure 2. EEG activity has been categorized as

ictal which is the phase during a seizure, the post-ictal the period after the seizure and the inter-ictal the period between seizures.

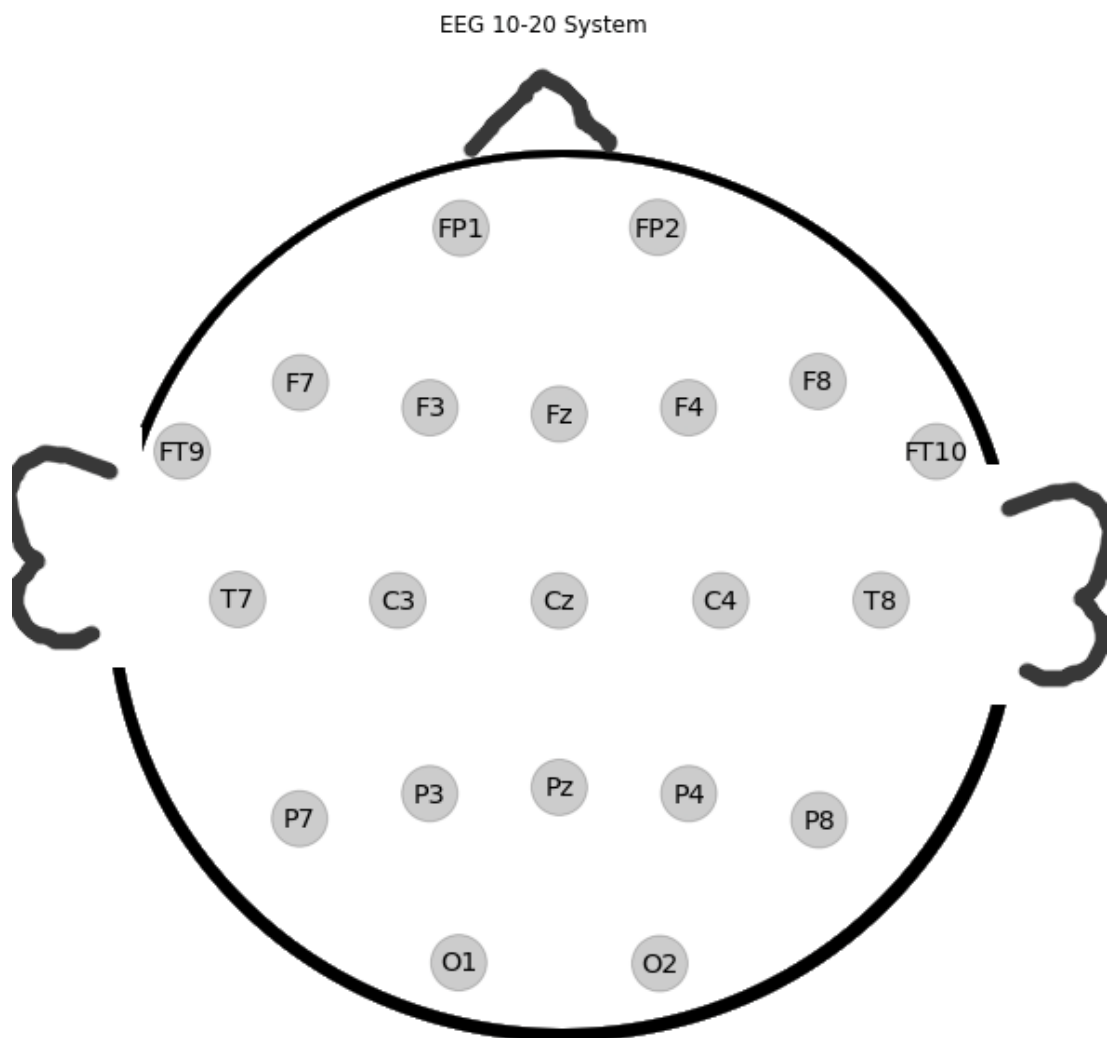


Figure 1. In this picture the positions of the electrodes on the scalp are placed according to the international 10-20 system that were used collecting the EEG data used in this work.

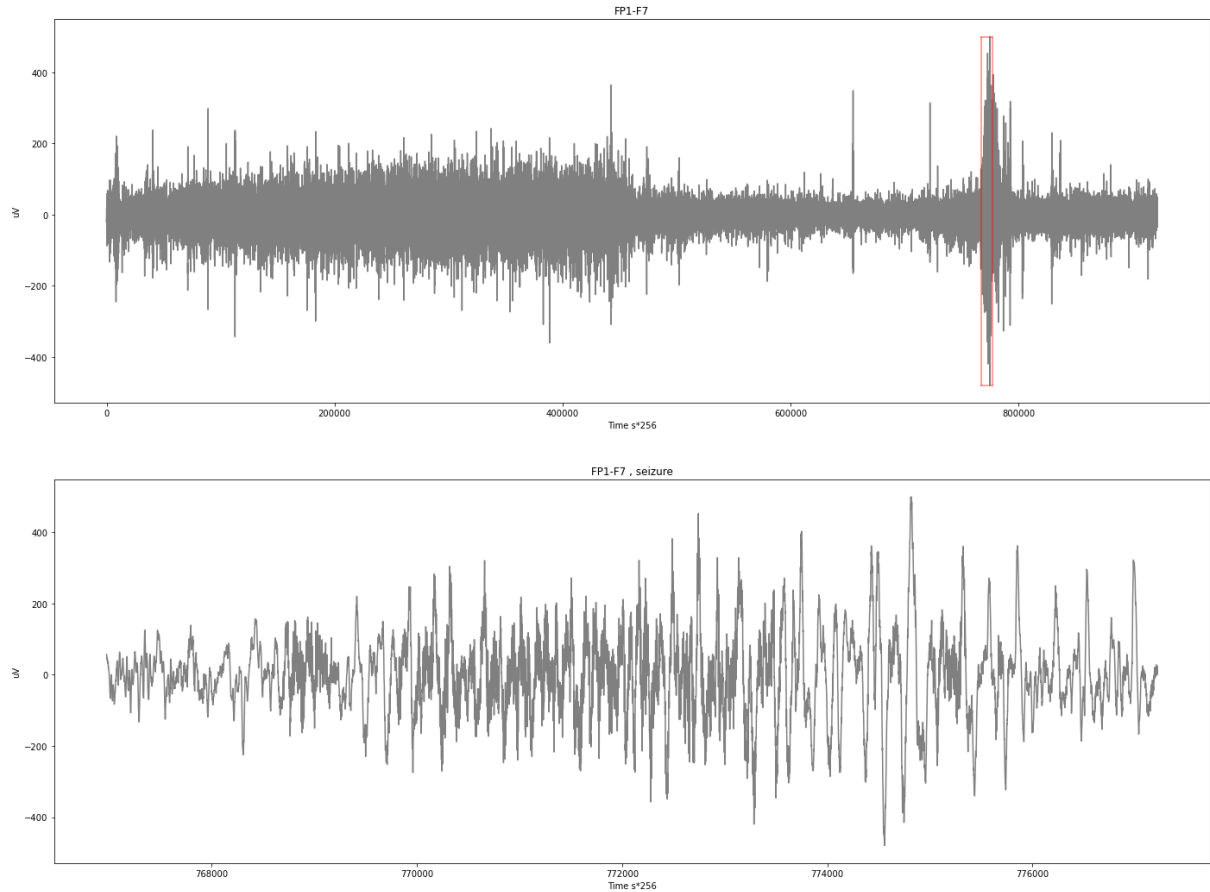


Figure 2. One of the EEG channel recordings of the patient file chb01_03, with the annotated seizure marked with red vertical lines (left panels). This is an example of the raw data and annotations. The panel title is the channel -- the signal is a voltage measured between the two electrodes (FP1 and F7). Note the number of non-seizure spikes, which make detection by voltage amplitude alone inaccurate. Right panel is a close-up of the seizure interval. The electrodes that comprise these channels are all on the left side of the scalp, as is indicated by having odd-number suffixes.

Mutual Information (MI)

Mutual Information quantifies how much information is shared between a pair of variables.

The information entropy $H(X)$ (in bits of information) of a variable x is given by the formula:

$$\text{Equation (1)} \quad H(X) = - \sum_{i=1}^n P(x_i) \log_2 P(x_i)$$

The joint entropy $H(X,Y)$ is given by the formula:

$$\text{Equation (2)} \quad H(X,Y) = - \sum_{i=1}^n P(x_i, y_i) \log_2 P(x_i, y_i)$$

This, combined with the entropy $H(X)$ and $H(Y)$, are used to calculate the Mutual Information $I(X;Y)$

$$\text{Equation (3)} \quad P_X(x) = \sum_y P_{XY}(x, y)$$

$$\text{Equation (4)} \quad I(X;Y) = \sum_{x,y} P_{XY}(x, y) \log_2 \frac{P_{XY}(x, y)}{P_X(x)P_Y(y)}$$

The Venn-diagram in figure 3 show the relationship between the Mutual Information $I(X;Y)$ and the entropies $H(X)$, $H(Y)$ and $H(X,Y)$.

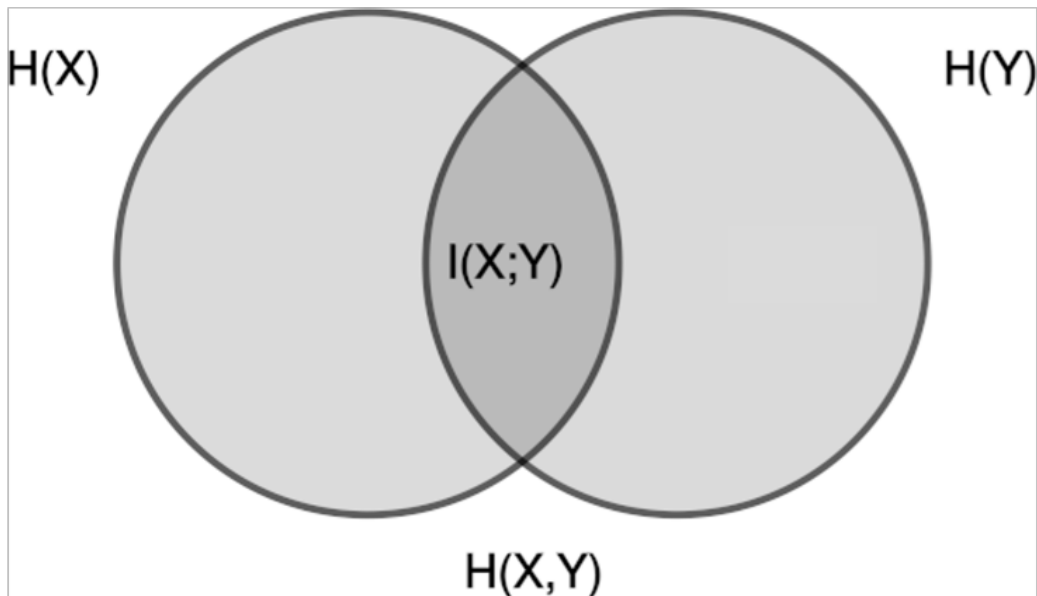


Fig 3. A Venn diagram showing the relationship between Mutual Information $I(X;Y)$, $H(X)$, $H(Y)$ and $H(X,Y)$.

Methods and material

EEG data

The raw data used in this work were taken from the CHB-MIT database [14] and contains multiple EEG recordings with and without seizures. EEG data were collected at the Children's Hospital, Boston for 23 pediatric patients. Data for one adult patient were collected at Beth Israel Deaconess Medical Center. Most of the data consists of 23 EEG channels and with the electrodes setup according to the international 10-20 system and recorded at 256 samples per second with a 16-bit resolution.

The data were first used in the publication “Application of Machine Learning To Epileptic Seizure Detection” by Ali Shoeb and John Guttag” [15] that made it available for download from the PhysioNet website: <http://physionet.org/physiobank/database/chbmit/>.

This dataset has been and are still frequently used in publications related to seizure detection and prediction. Since its public release a search in the PubMed database lists more than 70 references that have used this data set. Most of the data are recordings without seizures and with most seizures being short in time, seizures represent only 0.31% of the data in the recordings. No additional treatment than re-ordering, the removal of some channels (explained below) and truncation of digits were performed on the raw data. 16-bit numbers are (for our purposes) effectively continuous, whereas MI is computed on discrete data. One way to discretize is to truncate to use fewer digits. Artifacts of bias and noise were noted but kept as these are commonly observed in clinical practice.

Software

The algorithms used in this work was developed in Python 3.7.6 provided with the individual Anaconda distribution package (<https://www.anaconda.com>) for Macintosh and contains the SciPy libraries (<https://www.scipy.org>) and the scikit-learn libraries (<https://scikit-learn.org>) used for the calculation of MI. The import of raw data in EDF format was handled by the pyedflib-0.1.17 libraries for Python. The MI were be converted from the result from scikit-learn in units of nats (based on the natural logarithm, \log_e , \ln) into bits (based on \log_2) by dividing the result by $\log_e(2)$.

MI calculation

The raw-data files included channels that had no data or channels that were not present in all files and those were removed as mentioned. Most files contained duplicates of the channels T8-P8 and T7-P7 (P7-T7) which resulted in a MI biased towards those channels. The two duplicate channels measure the same property but a small difference in numerical values it gives an artifact of high mutual information that hides valuable information contributed by other paired EEG-channels. Additional channels found in some files but absent in others were removed to make as much of the raw data comparable. Only the 18 EEG channels present in all files were used in this work. MI were calculated by using a 10 second moving window that progressed with one second at time resulting in a 2560 x 18. matrix. As raw data were calculated on the separate files a gap of 9 seconds was introduced in the results of each calculated file (the sampling time).

Three main abbreviations of MI are used in this work:

- **MI_{tot}(t)** the sum of the mutual information over all channels, for a single moving window ending at time t.
- **MI_{t-ratio}(t)** = MI_{tot}(t) / MI_{tot}(t-Δt) where t is the current window time and t-Δt the previous window time, with Δt = 1s. This is a backward-difference discrete differentiation of MI_{tot}(t).

MI_{trn}(t) outputs 1 when MI_{t-ratio}(t) > ratio_lim for t, t-Δt, ..., t-(n-1)*Δt (in other words, for n successive seconds), and outputs 0 otherwise. Higher n reduces false positives, but also results in an n-1 second delay of an alert. A higher threshold (ratio_lim) reduces false positives, but also reduces sensitivity.

A large moving window acts as a low-pass filter, reducing the MI_{tot} as the proportion of new information introduced becomes less significant. It has fewer false positives, but more false negatives, in particular it tends to miss short seizures or seizures which generate low MI. A small moving window increase the number of short peaks with fairly high MI making noise within the raw data more significant. How the size of the moving window effects the type of peaks and thus peak finding are shown in the results section.

Bias in a graph of MI_{tot} by time is common. Peak detection is not performed against flat surroundings, and it is not necessarily the highest value of MI_{tot} that is related to a seizure. Rather we note that seizures are often associated with a rapid rise in MI_{tot} , hence our invention of the “rising-edge” based method $MI_{trn}(t)$. Detecting an onset of a seizure requires an algorithm that is able to discount the changes in MI_{tot} that are not related to seizures and instead detect the rapid increases of $MI_{tot}(t)$ that often characterize seizures. Normal brain activity and problems with the electrode measurements will always contribute to the overall MI_{tot} .

$MI_{t-ratio}$ and MI_{trn}

One expects $MI_{t-ratio} > 0$ on the rising edge of MI_{tot} . $MI_{trn}(t)$ returns 1 if $MI_{t-ratio}(t)$ exceeds the ratio_lim for nSAT (number of Seconds Above Threshold) consecutive seconds. In a clinical implementation this would sound an alert to staff.

Results

Calculating the Mutual Information between paired of EEG channels using a set window that progress with time during the recording of the EEG result in a graph of MI_{tot} windows by time where annotated seizures often are found as partially gaussian peaks. The length of the moving window defines the total MI as the amount of new information introduced are determine an increase or decrease of MI_{tot} . A rapid onset of a seizure will introduce a lot of information but have a smaller contribution in a large window. A too small window will enhance the contribution of all sources of information including noise and un-related seizure information. The balance of possible loss of information using a larger window giving more smooth peaks will affect peak finding but also delay it. In this work a 10 second moving window were used that progressed with 1 second. A smaller window size was not suitable for simple peak finding algorithms while a larger increased the risk of not detecting short seizures. I did not exhaustively evaluate the size of the moving window as using a 10 second window worked well. In figure 4 the effect of the size of using different sizes of the moving window is shown.

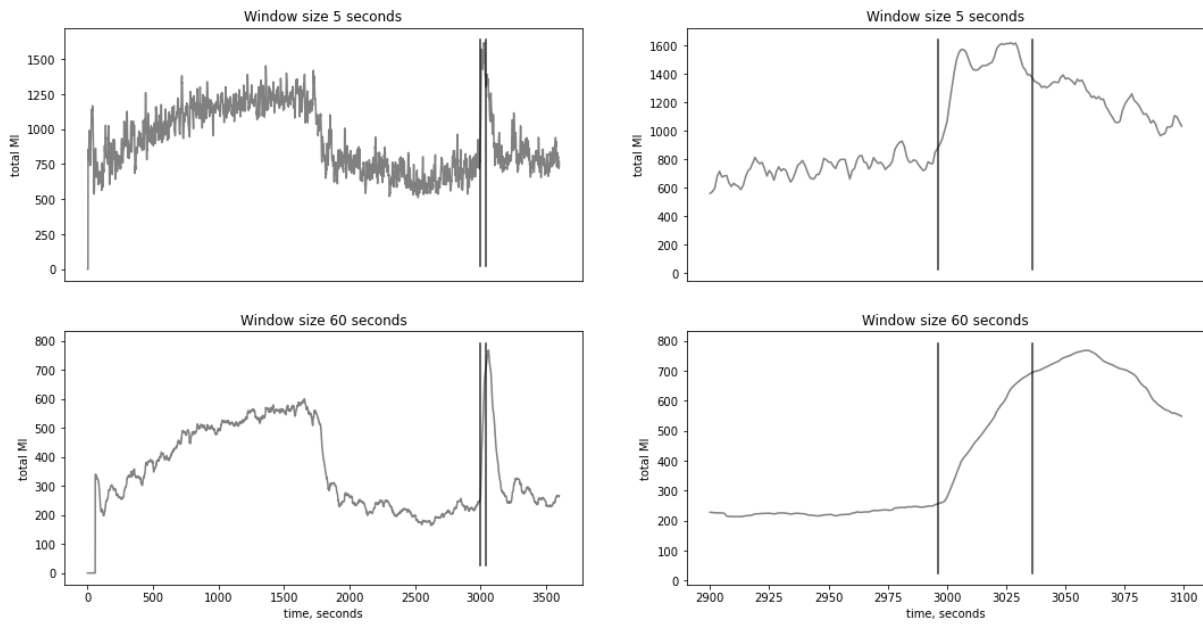


Figure 4. An example to illustrate how the chosen size for the moving window affects MI_{tot} . A 5 second (top) and 60 second (bottom) moving frame and the resulting $MI_{tot}(t)$ calculated for patient file chb01_03. The annotated seizure is marked with vertical lines in both panels. On the left is the entire recording and on the right is a close up of the seizure. Note the lower noise (hence fewer false positives) but also reduced amplitude (and potentially more false negatives) as well as delayed alert for the 60-second window.

As mentioned earlier duplicated EEG channels were present in most data files and were removed for making the data have a more equal contribution to MI_{tot} . Using data with no pre-filtering or alteration except for the truncation of digits has the advantage of being a fair evaluation of using MI with EEG. Removing artifacts in such complex raw data as EEG would enhance the overall statistic performance [15] but also require the knowledge of EEG recordings such as a trained physician has.

Detection results

Calculating the number of false-positive alarm rate per hour (FAR) is a fair judgement of the capability of predicting seizures [2, 15]. The prediction statistics for finding onsets of seizures were calculated based on the concatenation of the predicted results obtained from the patient files.

Larger gaps with missing recordings compared with time are the result of data files not being comparable and any offset related to the original data collection. The MI_{tot} and MI_{trn} were first calculated separately on each data-file, before the files were finally merged and the predictions were tabulated.

MI_{trn} was initialized as a test negative at the beginning of the recording. All possible seizure windows were checked against the record of annotated seizures (Gold Standard Positives). FP (False Positive), True Positive (TP), False Negative (FN), and True Negative (TN) were then tabulated based on the MI_{trn} result and Gold Standard annotation. The predictions were evaluated by calculating the accuracy, precision, sensitivity (True Positive Rate, TPR), specificity, and the False Positive Rate (FPR) for the individual patients and the concatenated (all-patient) results by the equations 5, 6, 7, 8 and 9 below. The performance was evaluated against several settings for the window size, ratio_lim, and nSAT defined earlier.

$$Equation \ (5) \quad Accuracy = \frac{TP + TN}{TP + FN + TN + FP}$$

$$Equation \ (6) \quad Precision = \frac{TP}{TP + FP}$$

$$Equation \ (7) \qquad \qquad \qquad Sensitivity \ (True \ Positive \ Rate) \ = \ \frac{TP}{TP + FN}$$

$$Equation \ (8) \qquad \qquad \qquad Specificity \ = \ \frac{TN}{TN + FP}$$

$$Equation \ (9) \qquad \qquad \qquad False \ Positive \ Rate \ = \ \frac{FP}{FP + TN}$$

The detection statistics are presented as a Receiver Operating Characteristic (ROC) calculated for the entire cohort of patient data. Based on the ROC curve a nSAT of 20 and the ratio_lim of 0.985, 0.995 and 1.005 were selected for the peak detection shown in figure 5. How the detection statistics are affected by different values of nSAT and the ratio_lim are shown in figure 6. A large nSAT are less effective for reducing the amount of FP than the ratio_lim. The FP drops significantly with a ratio_lim above 1 but also results in a lower TPR. It is also seen that the nSAT is less effective at a high or low ratio_lim and therefore can be adjusted to balance between a descent TPR and the delay of peak detection. The very steep slope when MI rise fast and are sustained for several seconds, the TPR rise faster than the FPR. An alarm can be created that take both the rate of rise of MI, and the number of seconds of that rise in consideration of detecting peaks. The effect of the nSAT and the ratio_lim and patient specificity are shown for the patients chb01 and chb15 in figure 7, figure 8 and figure 9. Patient chb15's seizures have been earlier reported as being difficult to detect by existing methods [15]. Our method MI_{trn} is able to detect the peaks related to the seizures as seen in figure 9. The MI_{tot} of chb15 is rather low compared to other patients and is apparently a patient specific characteristic. The numerical results for the entire concatenated cohort of patient files are found in table 1.

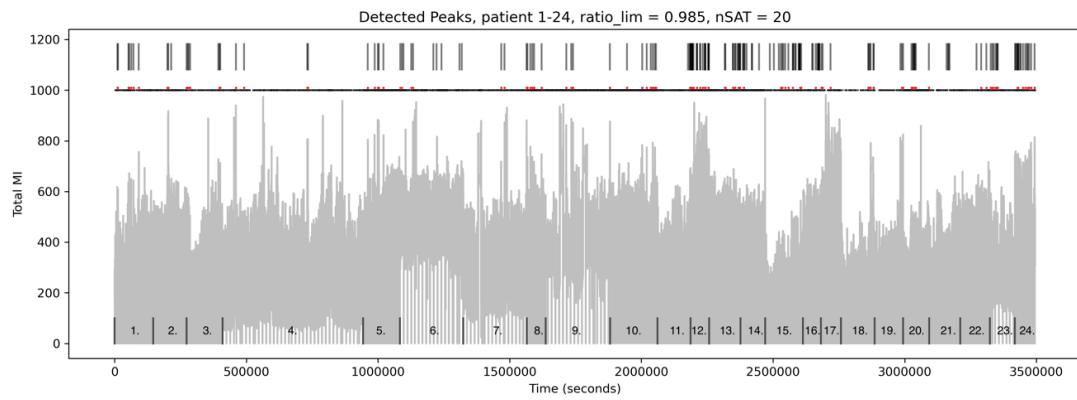


Figure 5 a.

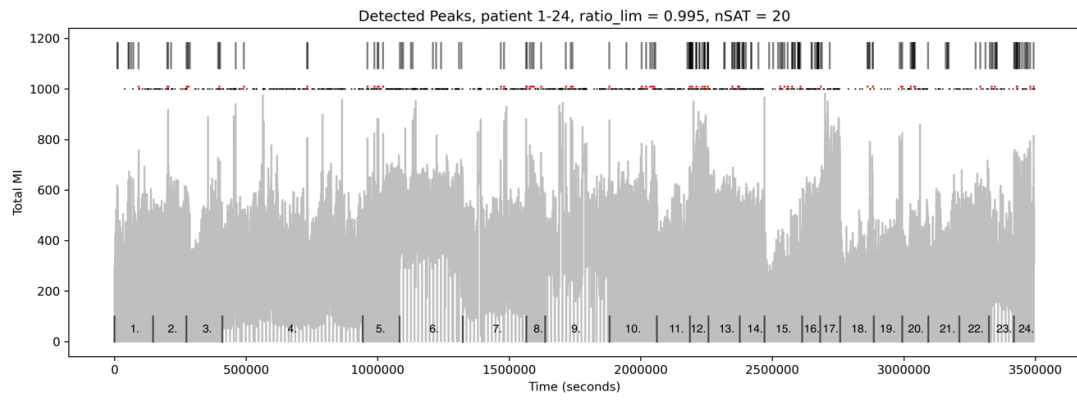


Figure 5 b.

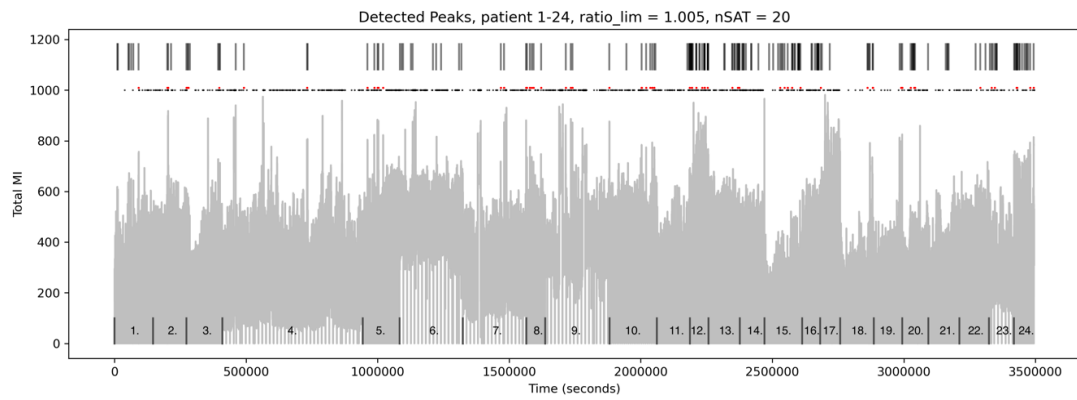


Figure 5 c.

Figure 5a – 5c. shows the concatenated MI of all patient files. The black vertical bars on top in the graphs represent the annotated seizures, while the black bars along the bottom axis indicate where each specific patient begins. The red colored dots are the MI_{trn} true positives and the black dots below false positives. The grey line is a visual artifact due to the ratio of 1:350 between seizure and non-seizures. At the bottom each patient number are shown between the vertical lines

ROC-curve, nSAT and Ratio_lim 0.8-1.05

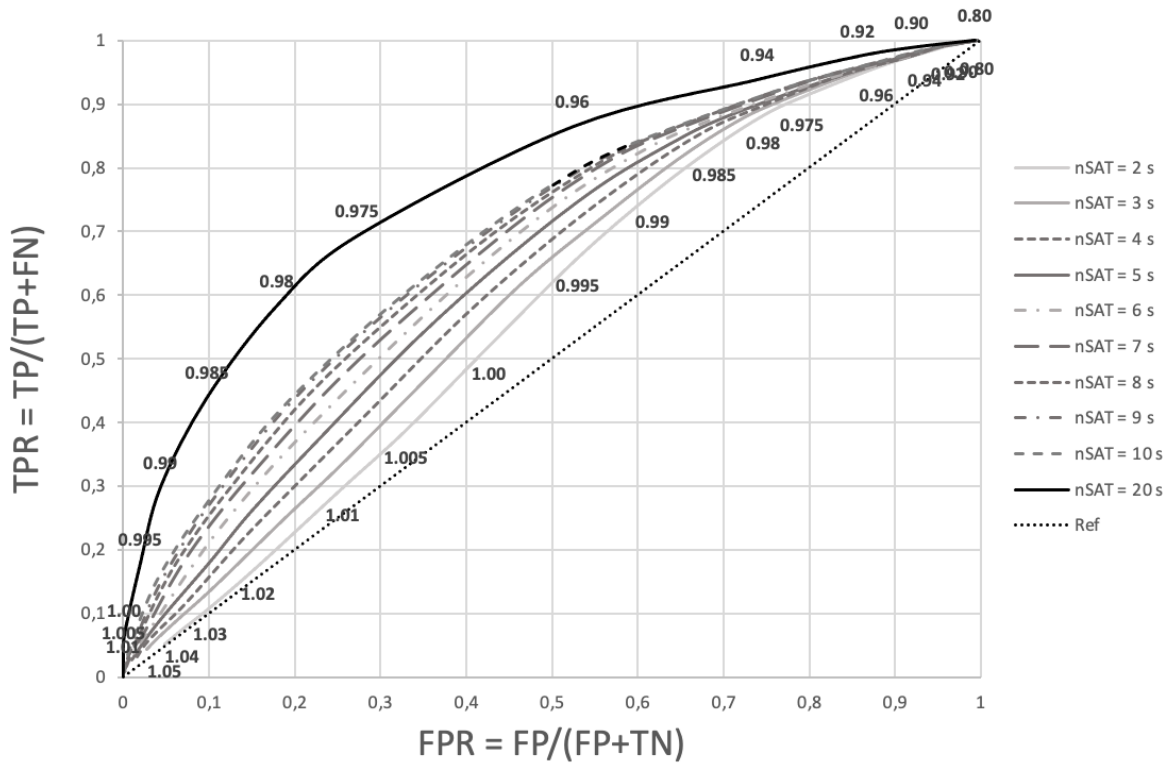


Figure 6. A ROC for all the patient results shows the drop of the FPR by changing the ratio_lim from 0.8 to 1.05 and the effect of the $nSAT$. The ratio_lim is marked in the graph for $nSAT$ equal with 2 and 20 seconds. $nSAT$ consecutive windows found with ratio_lim of 1.0 have a higher confidence of being a seizure, than if the ratio_lim were 0.975 for the same $nSAT$.

Table 2. Results for all patient data with varying nSAT and ratio_lim.

nSAT	ratio_lim	TP	FN	TN	FP	Accuracy	Precision	Sensitivity	Specificity	FPR	TPR (Sensitivity)
2	0.80	11028	4	15838	3468469	0.0076	0.0031	0.9996	0.0045	0.9954	0.9996
2	0.90	10980	52	80692	3403615	0.0262	0.0032	0.9952	0.0231	0.9768	0.9952
2	0.92	10937	95	131072	3353235	0.0406	0.0032	0.9913	0.0376	0.9623	0.9913
2	0.94	10817	215	226596	3257711	0.0679	0.0033	0.9805	0.065	0.9349	0.9805
2	0.96	10557	475	423254	3061053	0.1241	0.0034	0.9569	0.1214	0.8785	0.9569
2	0.975	10045	987	725891	2758416	0.2105	0.0036	0.9105	0.2083	0.7916	0.9105
2	0.98	9730	1302	882940	2601367	0.2553	0.0037	0.8819	0.2534	0.7465	0.8819
2	0.985	9183	1849	1082722	2401585	0.3123	0.0038	0.8323	0.3107	0.6892	0.8323
2	0.99	8381	2651	1333738	2150569	0.3839	0.0038	0.7596	0.3827	0.6172	0.7596
2	0.995	7263	3769	1637912	1846395	0.4706	0.0039	0.6583	0.47	0.5299	0.6583
2	1.00	5737	5295	1998319	1485988	0.5733	0.0038	0.52	0.5735	0.4264	0.52
2	1.005	4286	6746	2334565	1149742	0.6691	0.0037	0.3885	0.67	0.3299	0.3885
2	1.01	3285	7747	2592534	891773	0.7426	0.0036	0.2977	0.744	0.2559	0.2977
2	1.02	1935	9097	2935997	548310	0.8405	0.0035	0.1753	0.8426	0.1573	0.1753
2	1.03	1221	9811	3129621	354686	0.8957	0.0034	0.1106	0.8982	0.1017	0.1106
2	1.04	834	10198	3244358	239949	0.9284	0.0034	0.0755	0.9311	0.0688	0.0755
2	1.05	581	10451	3315931	168376	0.9488	0.0034	0.0526	0.9516	0.0483	0.0526
3	0.80	11028	4	15904	3468403	0.0077	0.0031	0.9996	0.0045	0.9954	0.9996
3	0.90	10980	52	85414	3398893	0.0275	0.0032	0.9952	0.0245	0.9754	0.9952
3	0.92	10935	97	140834	3343473	0.0434	0.0032	0.9912	0.0404	0.9595	0.9912
3	0.94	10803	229	247370	3236937	0.0738	0.0033	0.9792	0.0709	0.929	0.9792
3	0.96	10532	500	469835	3014472	0.1374	0.0034	0.9546	0.1348	0.8651	0.9546
3	0.975	9967	1065	819141	2665166	0.2372	0.0037	0.9034	0.235	0.7649	0.9034
3	0.98	9596	1436	1001612	2482695	0.2893	0.0038	0.8698	0.2874	0.7125	0.8698
3	0.985	8955	2077	1234624	2249683	0.3557	0.0039	0.8117	0.3543	0.6456	0.8117
3	0.99	8004	3028	1525053	1959254	0.4386	0.004	0.7255	0.4376	0.5623	0.7255
3	0.995	6793	4239	1870834	1613473	0.5371	0.0041	0.6157	0.5369	0.463	0.6157
3	1.00	5128	5904	2260644	1223663	0.6482	0.0041	0.4648	0.6488	0.3511	0.4648
3	1.005	3701	7331	2591686	892621	0.7425	0.0041	0.3354	0.7438	0.2561	0.3354
3	1.01	2748	8284	2827271	657036	0.8096	0.0041	0.249	0.8114	0.1885	0.249
3	1.02	1564	9468	3113106	371201	0.891	0.0041	0.1417	0.8934	0.1065	0.1417
3	1.03	1000	10032	3259878	224429	0.9329	0.0044	0.0906	0.9355	0.0644	0.0906
3	1.04	682	10350	3340950	143357	0.956	0.0047	0.0618	0.9588	0.0411	0.0618
3	1.05	476	10556	3388330	95977	0.9695	0.0049	0.0431	0.9724	0.0275	0.0431
4	0.80	11028	4	16015	3468292	0.0077	0.0031	0.9996	0.0045	0.9954	0.9996
4	0.90	10977	55	90682	3393625	0.029	0.0032	0.995	0.026	0.9739	0.995
4	0.92	10932	100	151703	3332604	0.0465	0.0032	0.9909	0.0435	0.9564	0.9909
4	0.94	10787	245	270730	3213577	0.0805	0.0033	0.9777	0.0776	0.9223	0.9777
4	0.96	10492	540	523054	2961253	0.1526	0.0035	0.951	0.1501	0.8498	0.951
4	0.975	9832	1200	923250	2561057	0.2669	0.0038	0.8912	0.2649	0.735	0.8912
4	0.98	9428	1604	1132319	2351988	0.3266	0.0039	0.8546	0.3249	0.675	0.8546
4	0.985	8704	2328	1397729	2086578	0.4023	0.0041	0.7889	0.4011	0.5988	0.7889
4	0.99	7651	3381	1724182	1760125	0.4954	0.0043	0.6935	0.4948	0.5051	0.6935
4	0.995	6273	4759	2096067	1388240	0.6014	0.0044	0.5686	0.6015	0.3984	0.5686
4	1.00	4573	6459	2493249	991058	0.7146	0.0045	0.4145	0.7155	0.2844	0.4145
4	1.005	3263	7769	2800228	684079	0.802	0.0047	0.2957	0.8036	0.1963	0.2957
4	1.01	2378	8654	3003079	481228	0.8598	0.0049	0.2155	0.8618	0.1381	0.2155
4	1.02	1288	9744	3230790	253517	0.9246	0.005	0.1167	0.9272	0.0727	0.1167
4	1.03	836	10196	3338542	145765	0.9553	0.0057	0.0757	0.9581	0.0418	0.0757
4	1.04	576	10456	3395636	88671	0.9716	0.0064	0.0522	0.9745	0.0254	0.0522
4	1.05	363	10669	3428144	56163	0.9808	0.0064	0.0329	0.9838	0.0161	0.0329

Table 1. Results for all patient data with varying nSAT and ratio_lim (continued)

nSAT	ratio_lim	TP	FN	TN	FP	Accuracy	Precision	Sensitivity	Specificity	FPR	TPR (Sensitivity)
5	0.80	11028	4	16135	3468172	0.0077	0.0031	0.9996	0.0046	0.9953	0.9996
5	0.90	10969	63	96362	3387945	0.0307	0.0032	0.9942	0.0276	0.9723	0.9942
5	0.92	10924	108	163327	3320980	0.0498	0.0032	0.9902	0.0468	0.9531	0.9902
5	0.94	10738	294	295969	3188338	0.0877	0.0033	0.9733	0.0849	0.915	0.9733
5	0.96	10404	628	580826	2903481	0.1691	0.0035	0.943	0.1666	0.8333	0.943
5	0.975	9709	1323	1033315	2450992	0.2984	0.0039	0.88	0.2965	0.7034	0.88
5	0.98	9225	1807	1267136	2217171	0.3651	0.0041	0.8362	0.3636	0.6363	0.8362
5	0.985	8470	2562	1561271	1923036	0.449	0.0043	0.7677	0.448	0.5519	0.7677
5	0.99	7306	3726	1913325	1570982	0.5494	0.0046	0.6622	0.5491	0.4508	0.6622
5	0.995	5840	5192	2297902	1186405	0.659	0.0048	0.5293	0.6595	0.3404	0.5293
5	1.00	4139	6893	2685863	798444	0.7695	0.0051	0.3751	0.7708	0.2291	0.3751
5	1.005	2894	8138	2959991	524316	0.8476	0.0054	0.2623	0.8495	0.1504	0.2623
5	1.01	2014	9018	3129159	355148	0.8958	0.0056	0.1825	0.898	0.1019	0.1825
5	1.02	1133	9899	3307327	176980	0.9465	0.0063	0.1027	0.9492	0.0507	0.1027
5	1.03	696	10336	3388174	96133	0.9695	0.0071	0.063	0.9724	0.0275	0.063
5	1.04	441	10591	3428165	56142	0.9809	0.0077	0.0399	0.9838	0.0161	0.0399
5	1.05	297	10735	3450430	33877	0.9872	0.0086	0.0269	0.9902	0.0097	0.0269
6	0.80	11028	4	16210	3468097	0.0077	0.0031	0.9996	0.0046	0.9953	0.9996
6	0.90	10964	68	102152	3382155	0.0323	0.0032	0.9938	0.0293	0.9706	0.9938
6	0.92	10901	131	175604	3308703	0.0533	0.0032	0.9881	0.0503	0.9496	0.9881
6	0.94	10710	322	322651	3161656	0.0953	0.0033	0.9708	0.0926	0.9073	0.9708
6	0.96	10337	695	640594	2843713	0.1862	0.0036	0.937	0.1838	0.8161	0.937
6	0.975	9573	1459	1143494	2340813	0.3298	0.004	0.8677	0.3281	0.6718	0.8677
6	0.98	9058	1974	1399529	2084778	0.4029	0.0043	0.821	0.4016	0.5983	0.821
6	0.985	8216	2816	1715942	1768365	0.4932	0.0046	0.7447	0.4924	0.5075	0.7447
6	0.99	6949	4083	2086248	1398059	0.5988	0.0049	0.6298	0.5987	0.4012	0.6298
6	0.995	5421	5611	2471203	1013104	0.7085	0.0053	0.4913	0.7092	0.2907	0.4913
6	1.00	3839	7193	2840078	644229	0.8136	0.0059	0.3479	0.8151	0.1848	0.3479
6	1.005	2654	8378	3079351	404956	0.8817	0.0065	0.2405	0.8837	0.1162	0.2405
6	1.01	1840	9192	3219605	264702	0.9216	0.0069	0.1667	0.924	0.0759	0.1667
6	1.02	950	10082	3359179	125128	0.9613	0.0075	0.0861	0.964	0.0359	0.0861
6	1.03	588	10444	3419241	65066	0.9783	0.0089	0.0532	0.9813	0.0186	0.0532
6	1.04	375	10657	3448474	35833	0.9866	0.0103	0.0339	0.9897	0.0102	0.0339
6	1.05	229	10803	3463937	20370	0.991	0.0111	0.0207	0.9941	0.0058	0.0207
7	0.80	11028	4	16264	3468043	0.0078	0.0031	0.9996	0.0046	0.9953	0.9996
7	0.90	10958	74	108266	3376041	0.0341	0.0032	0.9932	0.031	0.9689	0.9932
7	0.92	10895	137	188192	3296115	0.0569	0.0032	0.9875	0.054	0.9459	0.9875
7	0.94	10704	328	349645	3134662	0.103	0.0034	0.9702	0.1003	0.8996	0.9702
7	0.96	10315	717	700158	2784149	0.2032	0.0036	0.935	0.2009	0.799	0.935
7	0.975	9467	1565	1247824	2236483	0.3597	0.0042	0.8581	0.3581	0.6418	0.8581
7	0.98	8913	2119	1523302	1961005	0.4383	0.0045	0.8079	0.4371	0.5628	0.8079
7	0.985	7945	3087	1858015	1626292	0.5338	0.0048	0.7201	0.5332	0.4667	0.7201
7	0.99	6600	4432	2239523	1244784	0.6426	0.0052	0.5982	0.6427	0.3572	0.5982
7	0.995	5123	5909	2618211	866096	0.7505	0.0058	0.4643	0.7514	0.2485	0.4643
7	1.00	3516	7516	2962929	521378	0.8486	0.0066	0.3187	0.8503	0.1496	0.3187
7	1.005	2426	8606	3169519	314788	0.9074	0.0076	0.2199	0.9096	0.0903	0.2199
7	1.01	1673	9359	3285102	199205	0.9403	0.0083	0.1516	0.9428	0.0571	0.1516
7	1.02	809	10223	3395260	89047	0.9715	0.009	0.0733	0.9744	0.0255	0.0733
7	1.03	514	10518	3440941	43366	0.9845	0.0117	0.0465	0.9875	0.0124	0.0465
7	1.04	299	10733	3461934	22373	0.9905	0.0131	0.0271	0.9935	0.0064	0.0271
7	1.05	181	10851	3472577	11730	0.9935	0.0151	0.0164	0.9966	0.0033	0.0164

Table 2. Results for all patient data with varying nSAT and ratio_lim (continued)

nSAT	ratio_lim	TP	FN	TN	FP	Accuracy	Precision	Sensitivity	Specificity	FPR	TPR (Sensitivity)
8	0.80	11028	4	16348	3467959	0.0078	0.0031	0.9996	0.0046	0.9953	0.9996
8	0.90	10955	77	113737	3370570	0.0356	0.0032	0.993	0.0326	0.9673	0.993
8	0.92	10885	147	199865	3284442	0.0602	0.0033	0.9866	0.0573	0.9426	0.9866
8	0.94	10687	345	375836	3108471	0.1105	0.0034	0.9687	0.1078	0.8921	0.9687
8	0.96	10255	777	754628	2729679	0.2188	0.0037	0.9295	0.2165	0.7834	0.9295
8	0.975	9342	1690	1342773	2141534	0.3868	0.0043	0.8468	0.3853	0.6146	0.8468
8	0.98	8687	2345	1634677	1849630	0.4701	0.0046	0.7874	0.4691	0.5308	0.7874
8	0.985	7677	3355	1983292	1501015	0.5696	0.005	0.6958	0.5692	0.4307	0.6958
8	0.99	6318	4714	2371282	1113025	0.6802	0.0056	0.5726	0.6805	0.3194	0.5726
8	0.995	4852	6180	2739768	744539	0.7852	0.0064	0.4398	0.7863	0.2136	0.4398
8	1.00	3219	7813	3059771	424536	0.8763	0.0075	0.2917	0.8781	0.1218	0.2917
8	1.005	2178	8854	3237633	246674	0.9268	0.0087	0.1974	0.9292	0.0707	0.1974
8	1.01	1484	9548	3332968	151339	0.9539	0.0097	0.1345	0.9565	0.0434	0.1345
8	1.02	702	10330	3420864	63443	0.9788	0.0109	0.0636	0.9817	0.0182	0.0636
8	1.03	446	10586	3455552	28755	0.9887	0.0152	0.0404	0.9917	0.0082	0.0404
8	1.04	222	10810	3470530	13777	0.9929	0.0158	0.0201	0.996	0.0039	0.0201
8	1.05	82	10950	3477952	6355	0.995	0.0127	0.0074	0.9981	0.0018	0.0074
9	0.80	11028	4	16412	3467895	0.0078	0.0031	0.9996	0.0047	0.9952	0.9996
9	0.90	10947	85	118273	3366034	0.0369	0.0032	0.9922	0.0339	0.966	0.9922
9	0.92	10885	147	209377	3274930	0.063	0.0033	0.9866	0.06	0.9399	0.9866
9	0.94	10679	353	396308	3087999	0.1164	0.0034	0.968	0.1137	0.8862	0.968
9	0.96	10201	831	798310	2685997	0.2313	0.0037	0.9246	0.2291	0.7708	0.9246
9	0.975	9223	1809	1417382	2066925	0.4081	0.0044	0.836	0.4067	0.5932	0.836
9	0.98	8544	2488	1721422	1762885	0.4949	0.0048	0.7744	0.494	0.5059	0.7744
9	0.985	7477	3555	2081220	1403087	0.5975	0.0053	0.6777	0.5973	0.4026	0.6777
9	0.99	6111	4921	2473579	1010728	0.7094	0.006	0.5539	0.7099	0.29	0.5539
9	0.995	4637	6395	2831897	652410	0.8115	0.007	0.4203	0.8127	0.1872	0.4203
9	1.00	3010	8022	3133498	350809	0.8973	0.0085	0.2728	0.8993	0.1006	0.2728
9	1.005	1990	9042	3288877	195430	0.9415	0.01	0.1803	0.9439	0.056	0.1803
9	1.01	1346	9686	3368630	115677	0.9641	0.0115	0.122	0.9668	0.0331	0.122
9	1.02	623	10409	3438577	45730	0.9839	0.0134	0.0564	0.9868	0.0131	0.0564
9	1.03	367	10665	3465537	18770	0.9915	0.0191	0.0332	0.9946	0.0053	0.0332
9	1.04	158	10874	3476314	7993	0.9946	0.0193	0.0143	0.9977	0.0022	0.0143
9	1.05	49	10983	3481047	3260	0.9959	0.0148	0.0044	0.999	0.0009	0.0044
10	0.80	11028	4	16421	3467886	0.0078	0.0031	0.9996	0.0047	0.9952	0.9996
10	0.90	10947	85	119245	3365062	0.0372	0.0032	0.9922	0.0342	0.9657	0.9922
10	0.92	10885	147	211717	3272590	0.0636	0.0033	0.9866	0.0607	0.9392	0.9866
10	0.94	10670	362	402203	3082104	0.1181	0.0034	0.9671	0.1154	0.8845	0.9671
10	0.96	10179	853	811941	2672366	0.2352	0.0037	0.9226	0.233	0.7669	0.9226
10	0.975	9187	1845	1445741	2038566	0.4162	0.0044	0.8327	0.4149	0.585	0.8327
10	0.98	8482	2550	1757333	1726974	0.5051	0.0048	0.7688	0.5043	0.4956	0.7688
10	0.985	7379	3653	2124448	1359859	0.6099	0.0053	0.6688	0.6097	0.3902	0.6688
10	0.99	5967	5065	2523520	960787	0.7236	0.0061	0.5408	0.7242	0.2757	0.5408
10	0.995	4446	6586	2884158	600149	0.8264	0.0073	0.403	0.8277	0.1722	0.403
10	1.00	2795	8237	3179831	304476	0.9105	0.009	0.2533	0.9126	0.0873	0.2533
10	1.005	1840	9192	3324565	159742	0.9516	0.0113	0.1667	0.9541	0.0458	0.1667
10	1.01	1231	9801	3393724	90583	0.9712	0.0134	0.1115	0.974	0.0259	0.1115
10	1.02	552	10480	3451952	32355	0.9877	0.0167	0.05	0.9907	0.0092	0.05
10	1.03	275	10757	3472816	11491	0.9936	0.0233	0.0249	0.9967	0.0032	0.0249
10	1.04	102	10930	3479849	4458	0.9955	0.0223	0.0092	0.9987	0.0012	0.0092
10	1.05	40	10992	3482712	1595	0.9963	0.0244	0.0036	0.9995	0.0004	0.0036

Table 2. Results for all patient data with varying nSAT and ratio_lim (continued)

nSAT	ratio_lim	TP	FN	TN	FP	Accuracy	Precision	Sensitivity	Specificity	FPR	TPR (Sensitivity)
20	0.80	11028	4	24584	3459723	0.0101	0.0031	0.9996	0.007	0.9929	0.9996
20	0.90	10903	129	280716	3203591	0.0834	0.0033	0.9883	0.0805	0.9194	0.9883
20	0.92	10749	283	500166	2984141	0.1461	0.0035	0.9743	0.1435	0.8564	0.9743
20	0.94	10347	685	907645	2576662	0.2626	0.0039	0.9379	0.2604	0.7395	0.9379
20	0.96	9528	1504	1659253	1825054	0.4774	0.0051	0.8636	0.4762	0.5237	0.8636
20	0.975	7634	3398	2534663	949644	0.7273	0.0079	0.6919	0.7274	0.2725	0.6919
20	0.98	6430	4602	2859210	625097	0.8198	0.0101	0.5828	0.8205	0.1794	0.5828
20	0.985	4835	6197	3143744	340563	0.9007	0.0139	0.4382	0.9022	0.0977	0.4382
20	0.99	3282	7750	3332378	151929	0.9543	0.0211	0.2974	0.9563	0.0436	0.2974
20	0.995	1953	9079	3414593	69714	0.9774	0.0272	0.177	0.9799	0.02	0.177
20	1.00	707	10325	3479546	4761	0.9956	0.1292	0.064	0.9986	0.0013	0.064
20	1.005	330	10702	3482879	1428	0.9965	0.1877	0.0299	0.9995	0.0004	0.0299
20	1.01	84	10948	3483923	384	0.9967	0.1794	0.0076	0.9998	0.0001	0.0076
20	1.02	16	11016	3484300	7	0.9968	0.6956	0.0014	0.9999	0	0.0014
20	1.03	0	11032	3484307	0	0.9968	0	0	1	0	0
20	1.04	0	11032	3484307	0	0.9968	0	0	1	0	0
20	1.05	0	11032	3484307	0	0.9968	0	0	1	0	0

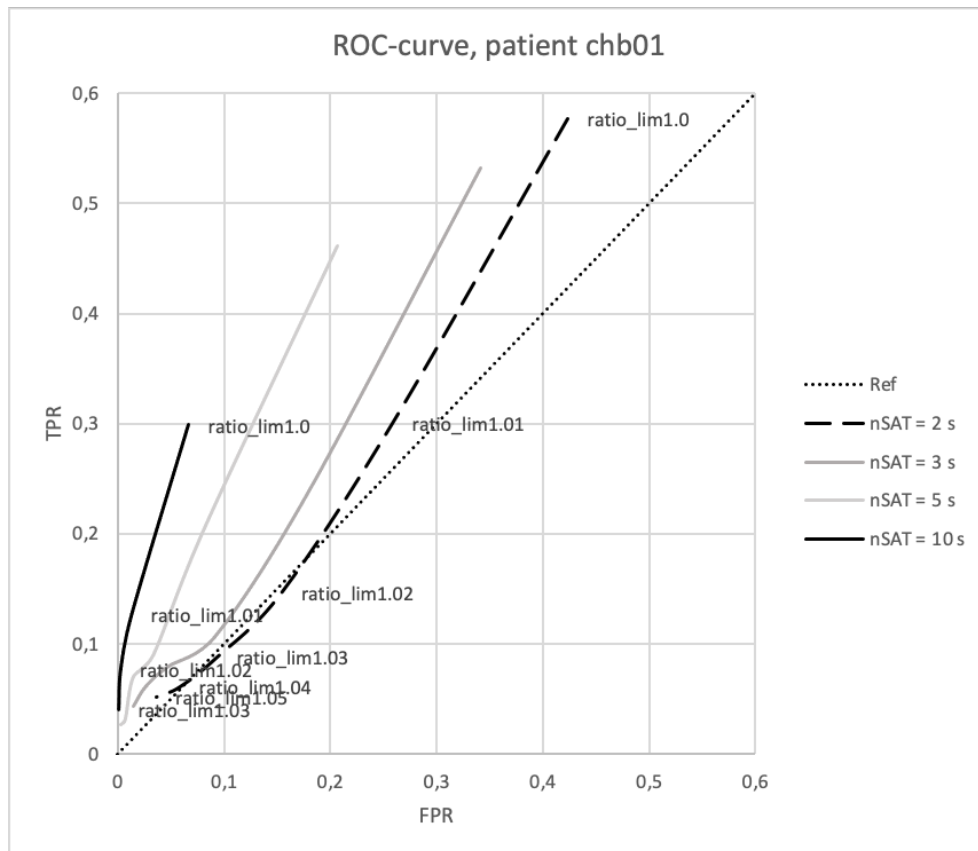


Figure 7. This ROC for patient chb01 shows the importance of balancing the ratio_lim and the nSAT using the MI_{trn} method. A high ratio_lim and high nSAT effectively lower the FPR but at the cost of the TPR.

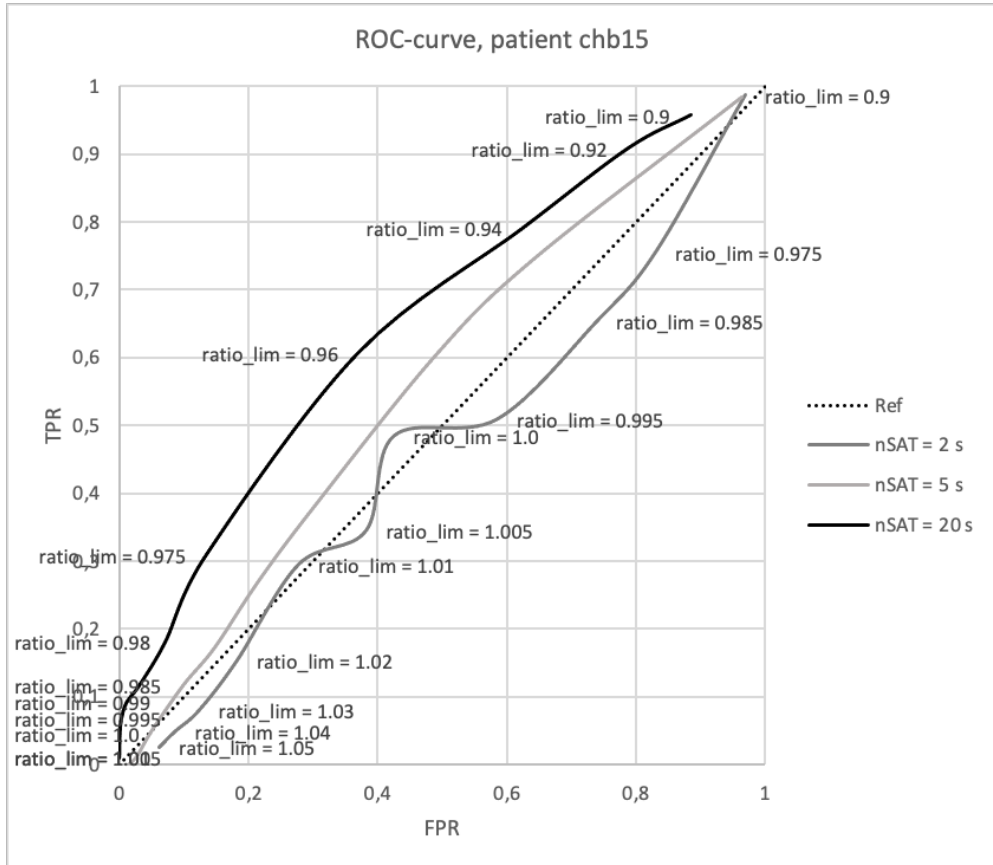


Figure 8. This ROC of patient chb15 shows that a low MI_{tot} can result in weaker seizure detection.

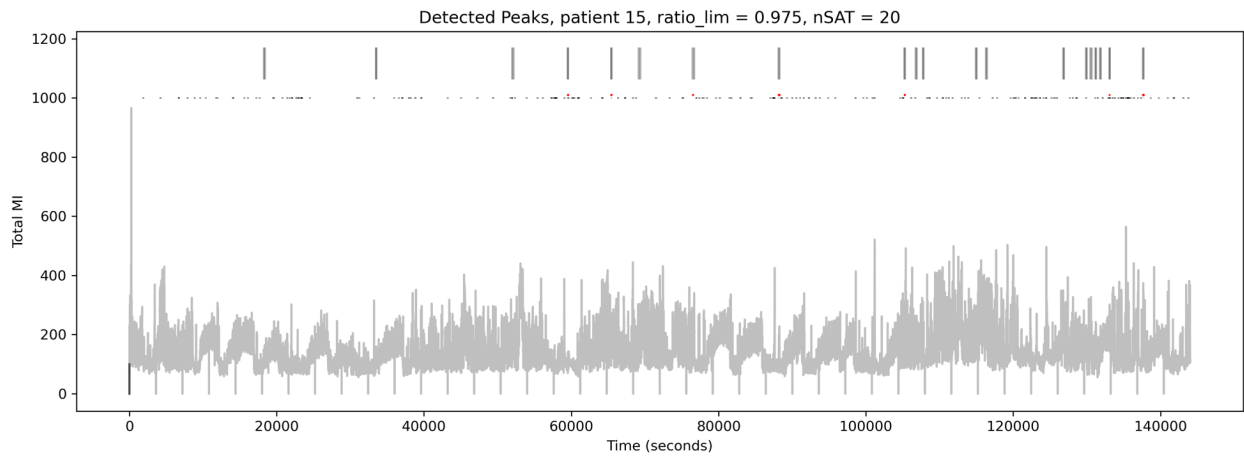


Figure 9. This graph shows patient chb15 even with a lower MI_{tot} than the other patients our MI_{trn} method are capable of detecting peaks (red dots) related to seizures. With a ratio of 1:72 between seizures and non-seizures the artifact of FP (blue dots) showing as a line is present.

Discussion

Our MI based method is capable of being used for detecting seizures in EEG data. Many methods used to detect and predict seizures based on the “chb mit EEG” data have been published and several are based on neural network approaches and signal processing [7, 14]. MI has been used as method for characterizing seizures in Alzheimer patients and also for comparison of data acquired with scalp electrodes and the ear-EEG “keyhole” proposing the use of small wearable ear EEG recorders [8, 16]. To our knowledge none have yet published a work using peak finding on MI and evaluated the possibility of using it for the detection of seizures. Seizure EEG channel patterns are known to be patient bound [2, 3, 5, 7, 10, 11, 13, 15] and it has been shown that single patients models perform better with less delayed alerts but that they also need individual adjustments [2, 6, 7, 10, 11, 15]. The visual benefit of calculating MI over time for an EEG and the using MI over time with peak finding algorithms has not been reported previously as a method for monitoring and detection of seizures. A method that is sensitive, fast, with a low rate of false alerts that are able to detect and monitor seizures defines an essential part of the ultimate seizure predictor [2, 3, 5, 6, 10, 11]. The method of seizure detection using MI as the main feature need hours of testing and development to show a better than chance performance a problem that most methods of seizure detection share. A lot of methods have failed when tested in practice while some based on NN looks promising [1, 4, 6, 10, 11].

MI shows clear benefits for application in monitoring seizure patients. MI_{tot} and MI_{trn} could be plotted vs. Time, in an easily understandable and interactive graphical user interface for an EEG device. The author is a former hospital chemist with a more than a decade of experience of diagnostic methods, connection of and evaluation of point of care (POC) instruments used daily by medical staff at the intensive care unit (ICU). Based on this experience, any method or application

must be easy and provide an interface that is understandable for the medical staff to use.

Monitoring real-time patient information from several systems (e.g. blood gases, glucose levels, and derived quantities) is routine at the ICU. One criterion of success for a point-of-care device is its easy visual interpretability, that will help medical staff in their decision making. Implementing MI as an addon for an EEG monitor would make EEG recordings more informative.

The algorithm used in this work associates the discrete derivative of MI, surpassing an adjustable threshold for an adjustable minimum of time, with the onset of a seizure. True Positives are computed as the dot product of test result vs. Gold standard annotation, rather than on a more sophisticated measure relating test result to seizure onset time. We argue that the latter measure will be more aligned with the intent of our algorithm, and report a higher TPR, but leave that for future work.

We have also tried Principal Components Analysis (PCA) to further reduce the amount of FP's and got promising results, but full validation of this is also left to future work.

References

1. Andrzejak R. G., Chicharro D., Elger C.E., Mormann F., Seizure prediction: Any better than chance? 2009, Clinical Neurophysiology, Volume 120, Issue 8, Pages 1465-1478
2. Baumgartner C., Koren J. P., 2018, Seizure detection using scalp-EEG. Epilepsia. 2018 June, 59 Suppl 1:14-22
3. Cook M. J., O'Brien T. J., Berkovic S. F., Murphy M., Morokoff A., Fabinyi G., D'Souza W., Yerra R., Archer J., Litewka L., Hosking S., Lightfoot P., Rueyebusch V., Sheffield W. D., Snyder D., Leyde K., Himes D., 2013, Prediction of seizure likelihood with a long-term, implanted seizure advisory system in patients with drug-resistant epilepsy: a first-in-man study, 2013, The Lancet Neurology, Volume 12, Issue 6, Pages 563-571
4. Elger C. E., Mormann F., 2013, Seizure prediction and documentation—two important problems, 2013, Volume 12, Issue 6, Pages 531-532
5. Freestone D. R., Karoly P. J., Peterson A. D., Kuhlmann L., Lai A., Goodarzy F., Cook M. J., 2015, Seizure Prediction: Science Fiction or Soon to Become Reality? Curr Neurol Neurosci Rep. 2015 Nov;15(11):73
6. Freestone D.R., Karoly P. J., Cook M. J., A forward-looking review of seizure prediction, 2017, Curr Opin Neurol 2017, 30:167 – 173
7. Hamavar R., Mohammadzadeh Asl B., 2021, Seizure onset detection based on detection of changes in brain activity quantified by evolutionary game theory model, Computer, Methods and Programs in Biomedicine, 2021, Volume 199, 105899
8. Jeong, J., Gore, J. C., Peterson, B. S., 2001, Mutual information analysis of the EEG in patients with Alzheimer's disease, 2001, Clinical Neurophysiology, Volume 112, Issue 5, Pages 827-835

9. Mikkelsen K. B., Kidmose P., Hansen L. K., 2017, On the Keyhole Hypothesis: High Mutual Information between Ear and Scalp EEG, *Frontiers in Human Neuroscience*, 2017, June 30, 341
10. Mormann F., Andrzejak R. G., 2016, Seizure prediction: making mileage on the long and winding road, 2016, Volume 139, 1622–1632
11. Mormann F., Andrzejak R. G., Elger C. E., Lehnertz K., 2006, Seizure prediction: the long and winding road, *Brain*, 2006, Volume 130, Issue 2, 314-333
12. PhysioNet website: <http://physionet.org/physiobank/database/chbmit/>.
13. Pinto M. F., Leal A., Lopes F., Dourado A., Martins P., Teixeira C. A., 2021, A personalized and evolutionary algorithm for interpretable EEG epilepsy seizure prediction. *Sci Rep.* 2021 Feb 9;11(1):3415.
14. Rukhsar S., Khan Y. U., Farooq O., Sarfraz M., Khan A.T., Patient-Specific Epileptic Seizure Prediction in Long-Term Scalp EEG Signal Using Multivariate Statistical Process Control, 2019, IRBM, Volume 40, Issue 6, Pages 320-331
15. Shoeb A., Guttag, J., 2010, Application of Machine Learning To Epileptic Seizure Detection, Proceedings of the 27 th International Conference on Machine Learning, Haifa, Israel, 2010.
16. Wei X., Zhou L., Zhang Z., Chen Z., Zhou Y., 2019, Early prediction of epileptic seizures using a long-term recurrent convolutional network, *Journal of Neuroscience Methods*, 2019, Volume 327, 108395

Acknowledgement

Huge thanks to Sam for coming up with the idea of using MI with EEG data. You saw the results I was to blind to see and that there were more than I needed for this thesis. I have no other excuse than I am a stubborn old man that don't know the value of splitting up results into several parts. Thanks for your belief in my atypical way of approaching and solving problems and that you never restricted my creativity. I am lucky that I have a supervisor that understand how my brain works when new ideas pop up. To be honest I had no idea I would not have returned to an office or lab being bored to death validating routine methods that describe almost three decades of my work experience. You gave me the chance to enjoy the less healthy coke containing corn syrup in USA and made my life contain an annual 25:th year experience of being an exchange student even if the one at age 50 were three weeks it brought back that extra needed feeling of happiness that I thought I would never feel again. Then you made me apply for that grant that resulted in this thesis. I have no words that can describe how grateful I am for all that you have done by not rejecting my academic skills as it is one of the reasons that has made me realized that leaving years of darkness behind and gain new knowledge was the right choice.

I also thank the Sven and Lily Lawska Foundation that made it possible for me a student that returned to the University after more than two decades in various laboratories to do another degree project and that allowed me to gain more knowledge of computational biology/chemistry.